

Machine Learning assisted Indoor Visible Light Communications Radio Environment Maps

Helena Serpi

*Department of Informatics and Telecommunications
University of Peloponnese*

Tripolis, Greece

e.serpi@uop.gr

Christina (Tanya) Politi

*Department of Electrical and Computer Engineering
University of Peloponnese*

Patras, Greece

tpoliti@uop.gr

Abstract—Visible light communications (VLC) have been proposed as reliable high-capacity wireless optical communication systems for indoor access networks. This technology comprises a solution that does not harm human tissues and has been especially suggested for ultra-reliable environments like hospitals. In this paper we utilize machine learning for investigating the wireless optical channel in indoor areas where ultra-reliable communications are needed and hence signal coverage should be guaranteed. It is proven that ML methods can reliably and efficiently predict the Radio Environment Map (REM) of a VLC enabled communication system.

Keywords—Visible Light Communications (VLC), Optical wireless channel modelling, Machine Learning

I. INTRODUCTION

Wireless optical communication systems, such as visible light communications (VLC) can provide reliable and secure platforms for high data rate indoor access networks compatible with 5th and 6th generation (5G and 6G) wireless networks [1, 2]. VLC technology that relies on modulation of Light Emitting Diodes (LEDs) for downlink and IR LEDs for up-link communication links, has been proposed for indoor access networks since light propagation is less prone to interference and less harmful for human tissues than all radio counterparts. Various systems have been proposed and IEEE has been working on standardization of VLC since 2009 as a strong candidate for Wireless Personal Area Networks (802.15), including full MAC and physical (PHY) layer protocols [3, 4].

Given VLC's advantage over radio technologies with respect to the effect on biological tissues, together with the latest advancements of the uplink and downlink systems, VLC is especially suitable for interconnecting the variety of ICT enabled medical technologies (from wearable sensors, to thermal cameras and from remote vital sign remote monitoring data to high-definition computer generated tomography) in a hospital environment. These devices may be interconnected to the processing units of the digital infrastructure through various wireless technologies and optical wireless technologies are suggested as the most suitable ones [5]. To that respect, using high-frequency pulsed light instead of radio frequencies and microwaves, VLC will enable the expansion of new medical applications, medical sensor monitoring and telemetry.

However, highly reliable and high-capacity health services pose stringent requirements for access network coverage, whether it is radio or light. Applying common network planning principles to investigate the reach of wireless technologies, implies identifying the characteristics of the area under study. These hospital areas may vary from remote,

isolated rooms, with challenging terrain for light coverage (e.g., large areas with big furniture, large medical equipment etc.) to long surgeries and corridors (e.g., with many curves, etc.). The rooms under study may even pose requirements for multiple access points in the same room. Considering the access network capacity, aggregate data rates of at least 300Mbps-1Gbps per room are required, and in cases that this is possible, data rates of 1-1.5 Gbps should be offered [6]. All the above are combined with stringent reliability requirements especially in the context of 5G ultra-reliable low latency communications (URLLC) services for hospital environments [5]. In order to address the requirements and KPIs, vast coverage and planning exercises must be performed, called optical radio environment maps, on versatile environments and areas to ensure that VLC access points operate sufficiently as ultra-reliable communications systems in places like hospitals and surgeries. In order to perform fast planning and delivery of those maps, various methods have been proposed that are based on analytical methods that lack accuracy.

In this paper, in order to overcome the high computation time needed for estimating the optical radio environment maps, i.e., specific metrics of the optical channel at each hospital room spot, we use machine learning (ML) methods. Initially we use a well-established indoor VLC channel propagation model to estimate the metric at a sub set of spatial points. Then we use these values to train our ML based system and predict values of the specified metric at each point of the hospital environment. We also evaluate the accuracy of various algorithms with respect to the expected simulated results using mean absolute error (MAE) as metric.

II. OPTICAL RADIO ENVIRONMENT MAPS

To operate ultra-reliable communications systems in places, like industrial areas and hospitals, Spectrum Cartography or Radio Environment Map (REM) is a helpful tool to gain knowledge about the radio channel of the area of interest [4]. REMs are databases of various radio channel metrics, e.g., RSS (Received Signal Strength), SINR, channel gain, at all known positions of the area under study. As channel propagation is determined by complex site-specific factors, a REM of a specific site can be constructed by measurements, e.g., a walking survey in a real environment or by model-based methods [8].

In an indoor VLC system, signal propagation characteristics depend on room geometry and specifications and transmitter/ receiver locations. Optical REMs are then constructed by estimating the RSS in all different locations of the areas for the VLC system under investigation. In this paper we use the multipath propagation model to calculate RSS values that is described in the following section.

III. INDOOR VLC CHANNEL PROPAGATION MODEL

VLC presents the potential of being used in both illumination and communication. Due to the incoherent characteristics of LEDs, intensity modulation with direct detection (IM/DD) is used where the information is encoded by varying the optical intensity of the transmitter ($x(t)$). The VLC transmitter consists of an array of LEDs that are intensity modulated by a baseband signal ($m(t)$). At the receiver terminal, the incident optical signal at the photo-detector is converted to an electrical signal through direct detection technique ($y(t)$). The output $y(t)$ can be calculated

$$y(t) = R \cdot x(t) \otimes h(t) + n(t) \quad (1)$$

$x(t)$ the optical intensity of the LED, is modulated by the input signal $m(t)$, $y(t)$ the photocurrent generated by the PD at the receiver and R is the PD responsivity, while $h(t)$ is the baseband CIR, \otimes denotes convolution, and $n(t)$ is the additive white Gaussian noise (AWGN).

Alternatively [9], the channel can be described in terms of the frequency response $H(f)$ which is the Fourier transform of $h(t)$

$$H(f) = \int_{-\infty}^{\infty} h(t) e^{-j2\pi ft} dt \quad (2)$$

We assume that the channel is distortionless, i.e., it has a gain $H(f) = H(0)$ for all frequencies of interest, while the zero-frequency (DC) value of the frequency responses can be expressed as

$$H(0) = \int_{-\infty}^{\infty} h(t) dt \quad (3)$$

The Path Loss of unshadowed diffuse configurations can be estimated using the expression [10]

$$RSS(dB) = PL_{Diffuse}(optical dB) = -10 \log_{10} \left(\int_{-\infty}^{\infty} h(t) dt \right) \quad (4)$$

Modelling of Single LED Case

In a standard empty room, the LED-based Tx is facing down and is placed on the center of the ceiling, while the PD-based Rx is facing upwards (Fig. 1). For the optical wireless channel, we consider both LoS (Line of Sight) and NLoS (Non-Line of Sight) transmission paths.

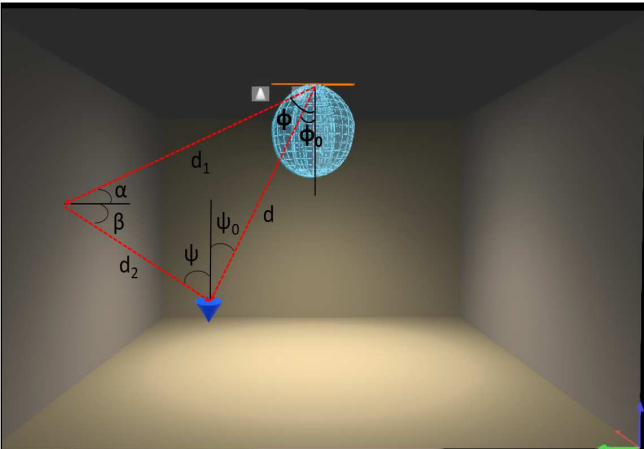


Fig. 1. VLC room configuration and LED placement with an indicative Lambertian radiation lobe with $m=1$. Two rays are shown as used in the multipath propagation model to calculate RSS.

The received intensity will depend on the emitter radiation pattern, the receiver optics, and the PD active area. Denoting the emitted optical intensity by P_T , the received optical power P_R is given by [11]

$$P_R = P_T H_{LOS}(0) + \int_{walls} P_T dH_{ref}(0) \quad (5)$$

We model the emitter by a generalized Lambertian pattern.

For the LOS path

$$H(0) = \begin{cases} \frac{(m+1)A_{PD}}{2\pi d^2} \cos^m(\varphi_0) T_s(\psi_0) g(\psi_0) \cos(\psi_0), & 0 \leq \psi_0 \leq \psi_c \\ 0, & \psi_0 > \psi_c \end{cases} \quad (6)$$

where m is the Lambertian order of the LED Tx (the directionality parameter of LED light)

$$m = \frac{-\ln 2}{\ln \cos(\Phi_{1/2})} = \frac{-\log_{10} 2}{\log_{10} \cos(\Phi_{1/2})} \quad (7)$$

and $\Phi_{1/2}$ is the semi-angle at half illuminance of the Tx (Half Power Angle), A_{PD} is the PD surface area, ψ_c is the Rx field of view (FOV) semiangle, and d is the distance from LEDs to the Rx point, $T_s(\psi_0)$ and $g(\psi_0)$ is the optical filter gain and the optical concentrator gain, respectively.

For NLOS path (single bounce reflection)

$$dH_{ref}(0) = \begin{cases} \frac{(m+1)A_{PD}}{2\pi d_1^2 d_2^2} \rho dA_{wall} \cos^m(\varphi) \cos(\alpha) \cos(\beta) T_s(\psi) g(\psi) \cos(\psi), & 0 \leq \psi \leq \psi_c \\ 0, & \psi > \psi_c \end{cases} \quad (8)$$

β represents the angle of irradiance from the reflective area of the wall, α is the angle of irradiance to the wall, d_1 and d_2 are the distances between the Tx and the wall, and the wall and a point on the receiving surface, respectively (Fig. 1), and dA_{wall} is the size of the reflective area, ρ is the reflection factor.

IV. INDOOR VLC RADIO ENVIRONMENT MAPS BASED ON MACHINE LEARNING (ML) REGRESSION METHODS

To overcome the high computation time needed for estimating the RSS value in each spot we use machine learning methods to train our system and predict RSS value at each point with coordinates (x, y, z) correctly.

Machine learning includes many tools that allow the interpretation and understanding of data through trained algorithms which reveal the correlations among the system's variables [8]. The main idea is to use a set of values for the target channel metric, RSS in our case, calculated for a set of locations and interpolate or extrapolate those input data to predict RSS values for another set of locations.

A. Generation of input values (input data set)

The system under investigation is a standard empty room with one LED Tx in the center of the ceiling (Fig. 2). In order to assess the performance of the ML regression methods, only single bounce reflections from the walls are considered. We modeled the VLC system in Matlab (version 2022a) [11] and calculated a large set of RSS values at random locations inside the room. Table I lists the values of key parameters used in the modelling of the hospital room.

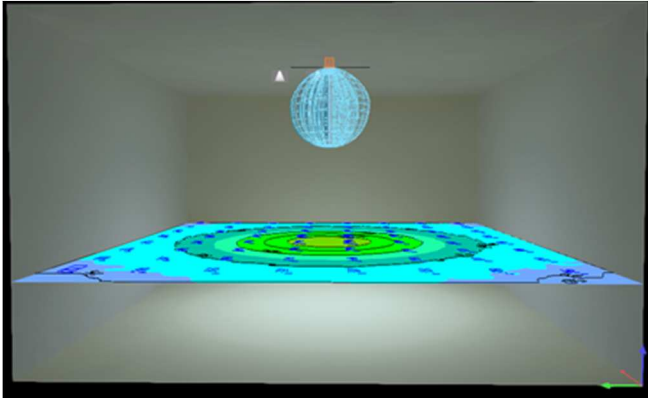


Fig. 2. Empty room illustration with LED Tx in the center of the ceiling and Rx plane at 1m height. The distribution of optical power is also illustrated.

TABLE I. MODELLING PARAMETERS OF SINGLE LED SYSTEM

Parameter	Value
Room size	5 x 5 x 3 m ³
Location of LED (T _x)	(2.5, 2.5, 3)
Area of PhotoDetector (PD)	10-4 m ²
Half Power Angle of T _x (HPA)	60°
Responsivity of PD	1.0
R _x 's Field of view (FOV)	85°
Transmitted power	1 W
Gain of optical filter	1.0
Refractive index of lens at the PD	1.5
Reflection factor of walls	0.8

B. Machine Learning methods

Machine Learning algorithms take as input the independent variables (features) of the system and train the ML model in order to categorize or predict the dependent variable [12]. In this work we used several supervised learning regression algorithms.

Support Vector Regression (SVR) is aiming to find decision boundaries (hyperplanes) to predict responses. Support Vectors are the data points closer to the hyperplane and determine its form and location. The best hyperplane is the one with maximum number of data points [13].

Decision Tree Regressor uses a set of splitting rules (resembling a tree) to segment the predictor space into a number of simple regions [14]. Decision trees exhibit instability in decisions even for small variations in data. To mitigate this, one can use Decision Trees within ensembles and reduce the variance of a decision tree base estimator.

The goal of ensemble methods is to combine the predictions of several base estimators (weak learners) and create a meta-algorithm with low bias and low variance [15]. There are three categories of ensemble methods, namely bagging, boosting and stacking.

In bagging, several estimators are built independently on random subsets of the original training set and their predictions are averaged. Random Forest and Extra-Trees are two bagging algorithms based on randomized decision trees [15].

In boosting, base tree estimators are built sequentially on repeatedly modified versions of the training data and the performance is improved iteratively by taking into account the prediction accuracy from the previous round. AdaBoost (adaptive boosting) algorithm [16] sequentially grows the weak learners (decision trees), learns from previous mistakes by assigning weights to incorrect values and combines the predictions from all trees through a weighted median to arrive to the final prediction.

Stacking is an ensemble machine learning algorithm that learns how to best combine the predictions from several weak learners using a meta-model. The selected meta-model is getting trained using the multiple predictions of the base models and produces the final prediction [17].

Hyper-parameters are the parameters used to construct an estimator. It is common practice the tuning of hyper-parameters of an estimator by searching the hyper-parameter space for the best cross-validation score [18].

C. Results and Discussion

We applied ML techniques to two different cases, the 2D and 3D case, respectively. The 2D case is being used as benchmark for an initial low complexity case. It is also typical in indoor wireless systems to estimate range at a specific level (eg desk level or person height). We started with the 2D case, where we generated RSS values at random locations of R_x on specific planes above the floor. Each input dataset refers to a different height of the plane layer. In the 3D case we calculated RSS values at random R_x locations inside the 3D room. The height of the random points is between zero (on the floor) and 1.7m to emulate a realistic hospital environment. So input datasets consist of either three or four columns. The first column comprises RSS values in dB calculated by (4), the second and third are the coordinates of the Rx location (x, y) on a plane with height (z) in the fourth column.

For the data analysis and visualization, we use the latest web-based interactive python development environment, JupyterLab [19], which is running on top of version 3.9.7 Python [20], and we implement various open source python libraries like pandas [21], numpy [22], scikit-learn [23] and matplotlib [24].

We split each dataset produced by simulation to two parts: 80% for training and 20% for testing and used these subsets to train and test the chosen ML regression algorithms. Then we applied the trained methods (prediction) to a completely different dataset of values which are considered as real values. Mean Absolute Error (MAE) is chosen as performance metric for all ML methods.

Table II shows the results of the ML regression for the 2D case in the plane at 1m height (Fig. 2). The input dataset to the ML algorithms consists of 10,000 rows while the dataset for value prediction has 2,500.

TABLE II. PERFORMANCE COMPARISON OF ML ALGORITHM MODELS FOR RSS PREDICTION IN TERMS OF MEAN ABSOLUTE ERROR (MAE) FOR RANDOM LOCATIONS OF TX ON THE PLANE AT 1M HEIGHT (2D CASE)

ML Regressor	Testing trained data (%)	Predicting data (%)
Support Vector	38.5	41.3
Decision Tree	8	15.5
Random Forest	8.4	18.3
Ada Boost with Extra Tree Regressor estimator	7.3	7.5
Stacking Regressor with XGB and LGBM estimators	2.8	14.3
Stacking Regressor with XGB, LGBM, Extra Tree, Random Forest and Decision Tree estimators	3	6.7

We design surface and contour plots of received power (dB) for R_x locations on the same plane (1m above the floor). The improvement of prediction between Support Vector and Ada Boost with Extra Tree Regressor estimator is clearly depicted in Fig. 3 and Fig. 4.

Best performance in 2D real data, with MAE 6.7%, is achieved with Stacking Regressor with XGB, LGBM, Extra Tree, Random Forest and Decision Tree estimators (Fig. 5).

The Mean Absolute Errors for the 3D case are shown at Table III. The input dataset consists of 75,000 rows while the dataset for value prediction has 25,000.

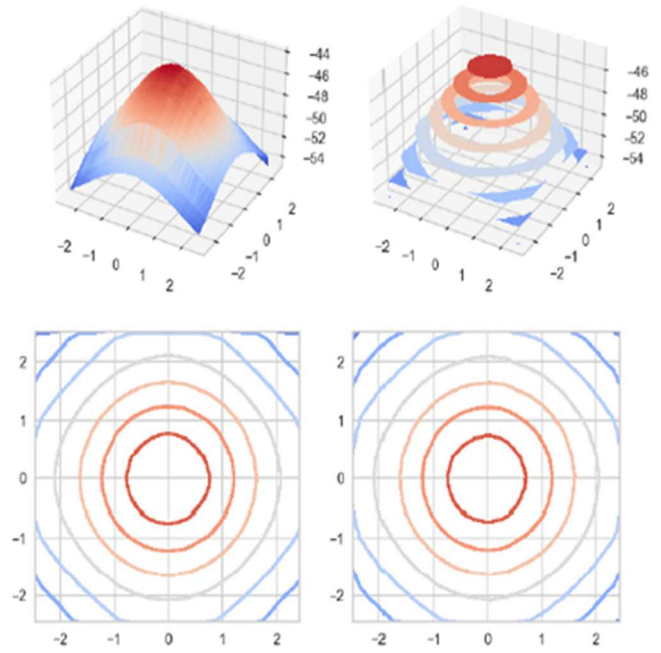


Fig. 4. Surface and contour plots of received power (dB) for R_x locations on the same plane (1m above the floor). On the left 2D real data, on the right predicted RSS values by Ada Boost with Extra Tree Regressor estimator.

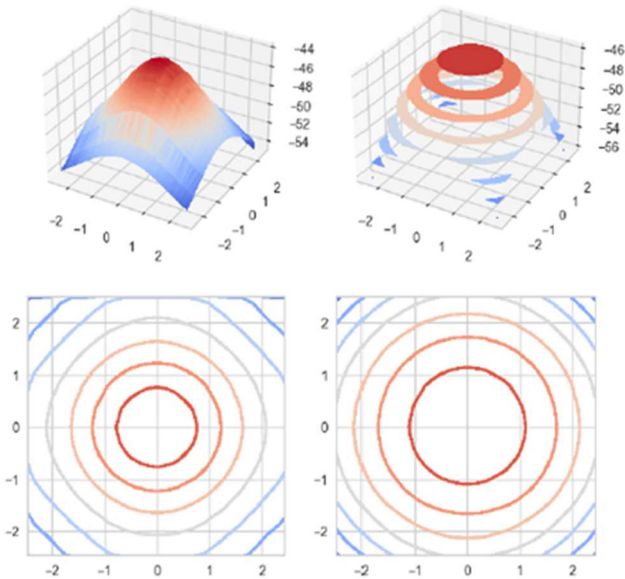


Fig. 3. Surface and contour plots of received power (dB) for R_x locations on the same plane (1m above the floor). On the left 2D real data, on the right predicted RSS values by Support Vector Regressor.

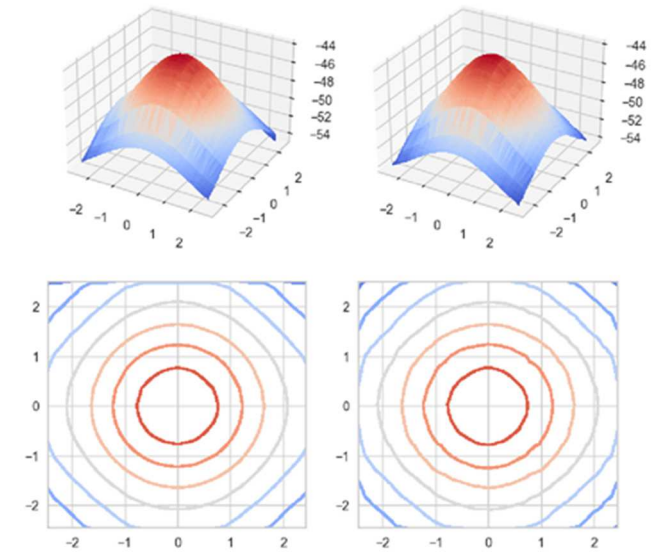


Fig. 5. Surface and contour plots of received power (dB) for R_x locations on the same plane (1m above the floor). On the left 2D real data, on the right predicted RSS values by Stacking Regressor with XGB, LGBM, Extra Tree, Random Forest and Decision Tree estimators.

TABLE III. PERFORMANCE COMPARISON OF ML ALGORITHM MODELS FOR RSS VALUES PREDICTION IN TERMS OF MEAN ABSOLUTE ERROR (MAE) FOR RANDOM LOCATIONS OF R_x IN THE ROOM (3D CASE)

ML Regressor	Testing trained data (%)	Predicting data (%)
Support Vector		
Decision Tree	16.4	25.3
Random Forest	20.2	25.5
Ada Boost with Extra Tree Regressor estimator	8.8	12.5
Stacking Regressor with XGB and LGBM estimators	6.8	18.9
Stacking Regressor with XGB, LGBM, Ada Boost with Extra Tree, Random Forest and Decision Tree estimators	4.8	18.9

To ensure that the most efficient ML method is proposed, Ada Boost with the Extra Tree Regressor estimator was applied at input datasets generated for two extra rooms, of different dimensions. The Mean Absolute Errors for the 3D case for rooms of $3 \times 3 \times 2.8$ and $6.5 \times 6.5 \times 3.5$ (with LED lamp at the center of the ceiling) are in the same range, that is 12.70% and 12.57%, respectively.

We plot 3D heatmaps (Fig. 6) to show performance of ML methods on predicting RSS values (dB) in random locations inside the room.

As soon as training has been performed prediction time for each RSS value at any location in the room ranges from 2 to 3ms, a value that is considered extremely low when compared to computation times of ray tracing numerical models (e.g., 1sec for one bounce reflections model, 94sec for 3 bounces and 197sec for five).

V. CONCLUSIONS

Radio Environment Maps (REMs) comprise a handy tool to gain knowledge about the radio channel of places like industrial areas, power plants, hospital environments etc., and helps to deliver fast network planning in order to achieve the requirements and KPIs in the context of 5G URLLC services in places of interest. Fast and accurate planning of a variety of places (e.g., different rooms in a hospital) is essential in ensuring service availability, hence tedious simulation of various environments is not favored. In this work we propose the use of ML assisted systems for obtaining fast, from 300 to 65000 times faster than calculating, depending on the number of reflections bounces considered, and accurate REMs for optical wireless systems like VLC. Initial results in predicting RSS values using R_x location as feature (predictor) showed a very promising accuracy performance measured by mean absolute error (12.5% MAE). In future work we seek to use more features, such as the HPA of T_x , the FOV of R_x , to improve accuracy by applying methods of artificial neural networks (ANN) and to create data sets publicly available.

ACKNOWLEDGMENT

H. S. and C.T.P would like to acknowledge Smart4All, a H2020-funded project (Grant Agreement No. 872614).

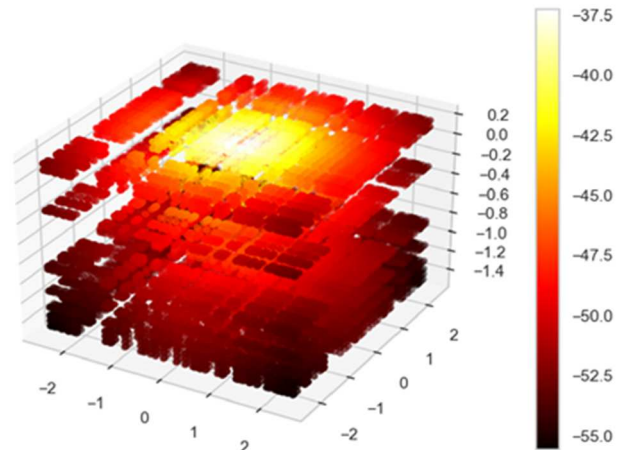
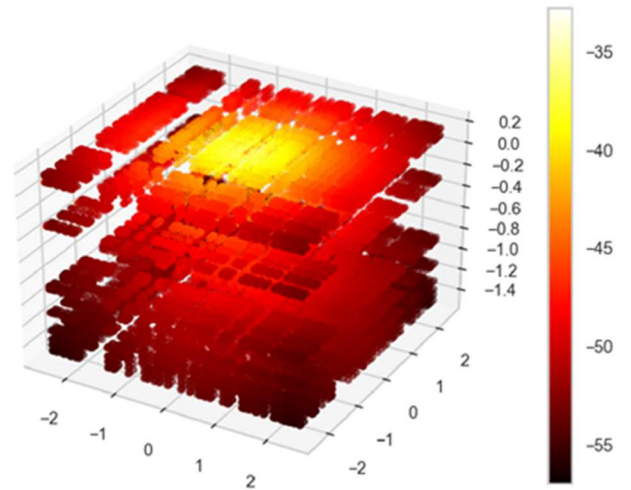


Fig. 6. Heatmap of received power (dB) in random locations inside the room. On top 3D real data and below predicted RSS values by Ada Boost with Extra Tree Regressor estimator.

REFERENCES

- [1] M. Ayyash *et al.*, "Coexistence of WiFi and LiFi toward 5G: concepts, opportunities, and challenges," *IEEE Communications Magazine*, vol. 54, no. 2, pp. 64–71, Feb. 2016, doi: 10.1109/MCOM.2016.7402263.
- [2] E. C. Strinati *et al.*, "6G: The Next Frontier: From Holographic Messaging to Artificial Intelligence Using Subterahertz and Visible Light Communication," *IEEE Vehicular Technology Magazine*, vol. 14, no. 3, pp. 42–50, Sep. 2019, doi: 10.1109/MVT.2019.2921162.
- [3] "IEEE Standard for Local and metropolitan area networks--Part 15.7: Short-Range Optical Wireless Communications," in IEEE Std 802.15.7-2018 (Revision of IEEE Std 802.15.7-2011), vol., no., pp. 1-407, 23 April 2019, doi: 10.1109/IEEESTD.2019.8697198.
- [4] <https://standards.ieee.org/ieee/802.11bb/10823/>, https://www.ieee802.org/11/Reports/tgbb_update.htm
- [5] I. Ahmed, H. Karvonen, T. Kumpulainen, and M. Katz, "Wireless Communications for the Hospital of the Future: Requirements, Challenges and Solutions," *Int J Wireless Inf Networks*, vol. 27, no. 1, pp. 4–17, Mar. 2020, doi: 10.1007/s10776-019-00468-1.
- [6] L. Mishra, Vikash, and S. Varma, "Seamless Health Monitoring Using 5G NR for Internet of Medical Things," *Wireless Pers Commun*, vol. 120, no. 3, pp. 2259–2289, Oct. 2021, doi: 10.1007/s11277-021-08730-7.
- [7] Y. S. Reddy, A. Kumar, O. J. Pandey, and L. R. Cenkeramaddi, "Spectrum cartography techniques, challenges, opportunities, and applications: A survey," *Pervasive and Mobile Computing*, vol. 79, p. 101511, Jan. 2022, doi: 10.1016/j.pmcj.2021.101511.
- [8] M. B. Kjærgaard, "A Taxonomy for Radio Location Fingerprinting," in *Location- and Context-Awareness*, vol. 4718, J. Hightower, B. Schiele, and T. Strang, Eds. Berlin, Heidelberg: Springer Berlin Heidelberg, 2007, pp. 139–156. doi: 10.1007/978-3-540-75160-1_9

- [9] J. M. Kahn and J. R. Barry, "Wireless infrared communications," *Proceedings of the IEEE*, vol. 85, no. 2, pp. 265–298, Feb. 1997
- [10] F. Miramirkhani, O. Narmanlioglu, M. Uysal, and E. Panayirci, "A Mobile Channel Model for VLC and Application to Adaptive System Design," *IEEE Communications Letters*, vol. 21, no. 5, pp. 1035–1038, May 2017, doi: 10.1109/LCOMM.2017.2651800.
- [11] Z. Ghassemlooy, W. Popoola, and S. Rajbhandari, *Optical wireless communications: system and channel modelling with MATLAB*, Second edition. Boca Raton, FL: CRC Press/Taylor & Francis Group, 2018.
- [12] A. Lionis, K. Peppas, H. E. Nistazakis, A. Tsigopoulos, K. Cohn, and A. Zagouras, "Using Machine Learning Algorithms for Accurate Received Optical Power Prediction of an FSO Link over a Maritime Environment," *Photonics*, vol. 8, no. 6, Art. no. 6, Jun. 2021, doi: 10.3390/photonics8060212.
- [13] N. Cristianini and J. Shawe-Taylor, *An Introduction to Support Vector Machines and Other Kernel-based Learning Methods*. Cambridge: Cambridge University Press, 2000
- [14] G. James, D. Witten, T. Hastie, and R. Tibshirani, *An introduction to statistical learning with applications in R: by Gareth James, Daniela Witten, Trevor Hastie, and Robert Tibshirani*, New York, Springer Science and Business Media, 2013.
- [15] T. Hastie, R. Tibshirani, and J. Friedman, *The Elements of Statistical Learning*. New York, NY: Springer New York, 2009. doi: 10.1007/978-0-387-84858-7.
- [16] Y. Freund and R. E. Schapire, "A Decision-Theoretic Generalization of On-Line Learning and an Application to Boosting," *Journal of Computer and System Sciences*, vol. 55, no. 1, pp. 119–139, Aug. 1997, doi: 10.1006/jcss.1997.1504.
- [17] L. Rokach, *Ensemble learning: pattern classification using ensemble methods*. World Scientific, 2019
- [18] Cross-validation: evaluating estimator performance, https://scikit-learn.org/stable/modules/cross_validation.html
- [19] <https://jupyter.org/>
- [20] <https://www.python.org/>
- [21] <https://pandas.pydata.org/>
- [22] <https://numpy.org/>
- [23] <https://scikit-learn.org/stable/>
- [24] <https://matplotlib.org/>